



Kinetics of the CO₂ gasification of woods, torrefied woods, and wood chars. Least squares evaluations by empirical models

Gábor Várhegyi¹ · Liang Wang² · Øyvind Skreiberg²

Received: 21 September 2022 / Accepted: 23 March 2023
© The Author(s) 2023

Abstract

The gasification kinetics of chars forming from biomass materials was studied by kinetic equations of type $dX/dt = A f(X) \exp(-E/(RT))$ where X is the conversion of the sample, A is the pre-exponential factor, E is the activation energy and $f(X)$ is a suitable model function. The theoretically deduced $f(X)$ models in the literature are rarely applicable for chars of biomass origin because of chemical and physical inhomogeneities and irregularities. Hence, empirical $f(X)$ functions were determined by a method proposed four years ago (Várhegyi in Energy Fuels 33:2348–2358, 2019). The parameters of the models were obtained by the method of least squares. Thermogravimetric experiments from an earlier work were reevaluated to explore the possibilities of the approaches employed. The experiments belonged to untreated birch and spruce woods; torrefied woods; chars prepared at a higher temperature; and chars formed at high heating rates (ca. 1400 °C min⁻¹). Common kinetic features were found for the CO₂ gasification of the chars studied. The reliability of the results was carefully tested by evaluating smaller and larger groups of the experiments and comparing the results. The method proved to be suitable for the determination of realistic $f(X)$, E , and A from single modulated experiments, too. The models described well the gasification of chars forming from different woods through a wide range of temperature programs and thermal pretreatments.

Keywords Kinetics · Least squares · Non-isothermal · Charcoal · Biomass · Wood

List of symbols

A/s^{-1}	Pre-exponential factor	N_{par}	The number of kinetic parameters in an evaluation
a_0, a_1, a_2	Polynomial coefficients in Eq. (7)	$p(X)$	Polynomial in Eqs. (2), (6) and (7)
c	Coefficient in Eq. (5)	of	The objective function to be minimized in the method of least squares
$E/kJ mol^{-1}$	The dimension of E is $kJ mol^{-1}$	R	Gas constant ($8.3143 \times 10^{-3} kJ mol^{-1} K^{-1}$)
$f(X)$	Function in Eq. (1)	$reldev/\%$	The root-mean-square deviation between the observed and calculated data expressed as per cent of the corresponding peak height
h_j/s^{-1}	Height of an experimental $-dm/dt$ curve in Eqs. (3) and (4)	$reldev_N/\%$	Root-mean-square of the $reldev$ values of N experiments
m	The mass of the sample normalized by the initial dry sample mass	t/s	Time
N	Number of the experiments evaluated together by the method of least squares	T	Temperature [°C, K]
M_j	The number of digital points in the j th experiment	X	Conversion (reacted fraction)

✉ Gábor Várhegyi
varhegyi.gabor@ttk.hu

¹ Institute of Materials and Environmental Chemistry, ELKH Research Centre for Natural Sciences, PO. Box 286, Budapest 1519, Hungary

² SINTEF Energy Research, Torgarden, Postboks 4761, 7465 Trondheim, Norway

Introduction

The char + CO₂ reaction is an important partial reaction of the biomass gasification processes [1, 2]. Besides, the char gasification by CO₂ may be a useful way for the utilization of various biomass wastes and residues [3–5]. The kinetics

of the char + CO₂ reaction is a fast-growing field of which extensive reviews are available [6–9].

The intrinsic kinetics of the char + CO₂ reaction is usually described by Eq. (1) in the kinetic regime, at a constant CO₂ concentration, and a low or negligible CO concentration:

$$dX/dt = Af(X)\exp\left(-\frac{E}{RT}\right) \quad (1)$$

Here X is the reacted fraction (conversion) while A and E are the pre-exponential factor and the activation energy. The reacted fraction is typically denoted by α in the other areas of the thermal analysis [10, 11]. The $f(X)$ function can be derived theoretically for high purity, idealistic carbons [12, 13]. Besides, other $f(X)$ functions derived for other sorts of idealized samples are also available [10]. However, the physical and chemical structure of the real chars are usually too complex for the idealized models. Note that the wood and biomass chars are formed from feedstocks that contain different compounds, different phases, and differently bound mineral matter. Moreover, the carbonization level of the char particles is not uniform because they are formed in furnaces or reactors in which the temperature distribution is uneven or not perfectly even. Accordingly, the $f(X)$ functions derived for ideal chars or for other idealized samples can only serve as semi-empirical or empirical models for the description of the real chars.

The kinetics of the CO₂ gasification of biomass materials needs further studies because the data reported in the literature showed a huge scatter even in the last few years. Chew et al., for example, reported activation energies of 15 kJ mol⁻¹ for the gasification of a torrefied palm kernel shell [14]. On the other hand, Sher et al. found $E = 544$ kJ mol⁻¹ for the gasification of a willow char [15]. To illustrate the unreality of these E values, let us consider the definition of the activation energy by IUPAC: “an empirical parameter characterizing the exponential temperature dependence of the rate coefficient” [16]. From this point of view, an activation energy of 15 kJ mol⁻¹ predicts nearly identical reaction rates at 800 and 900 °C while an activation energy of 544 kJ mol⁻¹ would correspond to reaction rates that differ by a factor of 181 at the same temperatures. The large scattering of the reported activation energies raises doubts about the reliability of the corresponding $f(X)$ functions, too.

The thermogravimetric analysis, TGA, is a suitable method to study the kinetics of the char gasification in the kinetic regime due to its high precision [7]. Usually the experiments are carried out either at isothermal or linearly increasing $T(t)$ functions (temperature programs). The present authors emphasized the use of other sorts of temperature programs, too, to obtain more experimental information [17–20]. Besides, it is difficult to carry out true isothermal

experiments in TGA. Typically, the gas is switched to CO₂ or to a CO₂—inert gas mixture after the heating to an isothermal temperature. Nearly, all works published in the present journal on CO₂ gasification used this method as illustrated by a selection in the References [21–25]. However, the stabilization of the CO₂ concentration in the furnace needs some time; it may take 20 min or even more [26, 27]. The increase of the CO₂ concentration after the gas switch results in an increasing reaction rate that may add a false maximum to the apparent $f(X)$ function. It is more accurate to set up the desired gas atmosphere below the gasification temperature and evaluate kinetically both the heat-up and the isothermal section. Note that suitable mathematical methods have been available for decades for the use of arbitrary $T(t)$ functions in the evaluations [28].

In our work we follow the so-called model fitting approach and evaluate more than one experiments together by the method of least squares as we have done in our earlier investigations [17–20, 29–33]. In the present article the examined process is described by Eq. (1). Várhegyi proposed versatile $f(X)$ functions for Eq. (1) in 2019 [30]. Their applicability as empirical models were extensively tested on TGA experiments from earlier studies on the thermal decomposition of biomasses [30, 31], char combustion [32], and char gasification [33]. The corresponding kinetic equation can be written as

$$dX/dt = \exp\left[p(X) - \frac{E}{RT}\right](1 - X) \quad (2)$$

where $p(X)$ is a polynomial. The term $(1-X)$ ensures that dX/dt is zero at $X = 1$ for any polynomial coefficients. Equation (2) can be rewritten into the form of Eq. (1) as outlined in section “Materials and methods”. Equation (2) can be solved numerically for the $T(t)$ functions of the experiments. The polynomial coefficients of $p(X)$ can be determined by the method of least squares ensuring that the experimental data and their counterparts calculated from the model would be close to each other [30–33].

In the present work we continued the exploration of the properties and possibilities of this type of modelling. An earlier set of experimental data of the authors [19] was reevaluated by this newer modelling tool. Two woods were examined of which chars were formed through a particularly wide range of temperature histories. These latter included torrefaction at two temperatures; slow heating till 700 °C; fast heating (ca. 1400 °C min⁻¹) till 700 °C; and a one-hour carbonization at 750 °C. The aim was to find the common kinetic features for the gasification of these chars in the kinetic regime. Besides, the reliability of the employed methods and the obtained results was also carefully tested. This is a crucial point in all evaluations of experiments [34]. However, the methods of the mathematical statistics are not

suitable for assessing the reliability of the results because the major experimental errors are neither random and nor independent in thermal analysis [18]. Accordingly, a different approach was used which is described below, in section “Tests on the reliability of the results”.

Materials and methods

About the experiments reevaluated

As mentioned in the Introduction, the present work is based on the experiments of an earlier study of the authors [19]. The detailed description of the materials and experiments can be found in that work. A summary is given here to help and orient the readers of the present work. The CO₂ gasification of woods and torrefied woods was studied in a TGA apparatus. For comparison, two chars prepared at 750 °C were also included into the study. The notation of the samples refers to the type of wood (B for birch and S for spruce), followed by three digits that refer to the temperature of the torrefaction (225 and 275 °C) or carbonization (750 °C). These digits are obviously missing for the untreated woods, which are denoted by B— and S—. During the TGA experiments the samples were heated in a CO₂ gas flow from room temperature till 1000 °C with a drying section at 120 °C. Three different temperature programs were employed for each sample: a linear $T(t)$ with a heating rate of 20 °C min⁻¹; a modulated experiment where a sine function with 5 °C peak amplitude and 200 s wavelength was added to a 5 °C min⁻¹ linear $T(t)$; and a constant reaction rate (CRR) $T(t)$. In the CRR experiments, the equipment regulated the heating of the samples so that the reaction rate would remain below a preset limit. The latter was 2 μg/s in the experiments treated here. Besides, additional experiments were carried out to check how the heating rate of the devolatilization section influences the gasification of the formed chars. For this purpose, TGA experiments were carried out with a particularly slow (2 °C min⁻¹) and a particularly fast heating rate (ca. 1400 °C min⁻¹) until 700 °C. The sample was kept at 700 °C for 3 min in these experiments and was heated by 20 °C min⁻¹ afterward [19]. These experiments were also included into the kinetic evaluation.

The method of least squares

As outlined in the Introduction, the evaluation is based on Eq. (2). The parameters of this empirical model were determined so that the distance between the measured and the calculated data would be minimal. The root-mean-square deviation normalized by the highest experimental value can serve as a measure of this distance for a given experiment.

We shall express it as a percent of the highest experimental value:

$$reldev(\%) = 100 \left\{ \sum_{i=1}^{M_j} \frac{\left[\left(\frac{dm}{dt} \right)_j^{obs}(t_i) - \left(\frac{dm}{dt} \right)_j^{calc}(t_i) \right]^2}{M_j h_j^2} \right\}^{0.5} \quad (3)$$

Here M_j is the number of points available in digital form for experiment j , m is the normalized sample mass, and h_j is the highest value of the observed mass loss rate, $-(dm/dt)_j^{obs}$. The fit quality of N experiments is characterized by the root-mean-square of the corresponding $reldev$ values and is denoted by $reldev_N$. When N experiments are evaluated together, such parameters are searched for which $reldev_N$ is minimal. This can be achieved by minimizing $(reldev_N)^2$ by the method of least squares, i.e., to use an objective function defined by Eq. (4):

$$of = \sum_{j=1}^N \sum_{i=1}^{M_j} \frac{\left[\left(\frac{dm}{dt} \right)_j^{obs}(t_i) - \left(\frac{dm}{dt} \right)_j^{calc}(t_i) \right]^2}{M_j h_j^2} \quad (4)$$

The numerical solution of the kinetic equation, Eq. (2), provides $(dX/dt)^{calc}$ values which are proportional to the $(-dm/dt)^{calc}$ values:

$$(-dm/dt)^{calc} = c(dX/dt)^{calc} \quad (5)$$

Here c is a constant characteristic to the given experiment. It is equal to the total mass-loss during the gasification normalized by the initial sample mass [19]. The value of c cannot be calculated directly from the TGA data because the last part of the devolatilization overlaps with the start of the gasification, hence we do not know what the sample mass is exactly at the beginning of the gasification. Accordingly c is an unknown parameter which is determined together with the other parameters by the method of least squares [19]. One cannot assume common c values for a group of experiments because the amount of formed char depends on the temperature program in the case of biomass materials [35]. We can envisage c as a scale factor: during the evaluation the program scales the calculated $(dX/dt)^{calc}$ curves to the corresponding experimental $(-dm/dt)^{obs}$ curves for each set of kinetic parameters by calculating the best fitting c values by a simple formula shown in the Supplementary Information. Therefore, the c values are not regarded as kinetic parameters.

The description of the applied numerical methods can be found in our earlier works [30, 33]. Some aspects of the calculations are also explained in Sect. 4 of the Supplementary Information.

The model

As mentioned in the Introduction, the work is based on Eq. (2) which is a special case of Eq. (1). A simple rearrangement of Eq. (2) yields the $Af(X)$ term [33]:

$$Af(X) = e^{p(X)}(1 - X) \quad (6)$$

Equation (6) provides a smooth function with zero at $X = 1$ for any polynomial coefficients. It can be factorized into an A value and an $f(X)$ function if $f(X)$ is normalized. A simple, straightforward normalization is to require the $f(0) = 1$ equality [33]. If $p(X)$ is expressed as

$$p(X) = a_0 + a_1X + a_2X^2 + \dots + a_nX^n \quad (7)$$

then, obviously, $Af(0) = e^{a_0}$, hence the $f(0) = 1$ normalization results in $A = e^{-a_0}$. Accordingly, the kinetic parameters to be determined are E , A , and polynomial coefficients a_1, a_2, \dots, a_n . In the actual calculations the polynomials were represented by finite Chebyshev series to decrease the compensation effects between the polynomial coefficients during the minimization of the least squares sum [30, 32, 33, 36], and the coefficients of the Chebyshev polynomials were determined by the method of least squares. (See the explanations in section 4.2 of the Supplementary Information.)

In the present work 5th order and 7th order polynomials were tested for $p(X)$. There were no mentionable differences between the use of 5th order and 7th order polynomials from a computational point of view. However, the reliability tests with 7th order polynomials gave more favorable results (i.e., less scatter in the obtained activation energies and $f(X)$ functions) than the 5th order polynomials. Accordingly, the 7th order results are presented in the paper. The previous works with this type of modelling revealed that the employing of higher polynomials did not cause any problems: the unnecessary terms in the polynomials became insignificant when they were not needed [32]. This was so in the present work, too. An example is shown in section. 4.4 of the Supplementary Information.

Results and discussions

Determining an $f(X)$ function and an activation energy value for the samples of a given feedstock

In this evaluation the experiments belonging to a given feedstock were evaluated together by the method of least squares assuming a common E and a common $f(X)$ for the corresponding samples. The notation of the evaluations

in this paper indicates the number of $f(X)$ functions and E values for the whole set of experiments. Accordingly, the evaluation treated in this section is denoted by $[2 f(X); 2 E]$.

It is known that the thermal pretreatments as well as the temperature programs of the experiments affect the reactivity of the char forming from biomass materials and influences the thermal deactivation (annealing) at temperatures of the gasification [35, 37, 38]. As an approximation, the corresponding changes in the reactivity can be described by the pre-exponential factors. Accordingly, the pre-exponential factors varied from experiment to experiment. We return to this point in a later section of the paper as well as in the Supplementary Information.

Figure 1 illustrates the obtained fit qualities: the best, the worst and a typical fit qualities are shown for the birch and the spruce samples. Circles represent the calculated curves of this evaluation.

The main characteristics of the $[2 f(X); 2 E]$ evaluations are listed in Table 1. There are eight common kinetic parameters in this evaluation: seven polynomial coefficients for the $f(X)$ function (as explained in section “Materials and methods”), and one activation energy. Their determination for the samples of a given feedstock was based on N experiments. As outlined above, there is a separate pre-exponential factor for each experiment. Hence the number of parameters to be determined, N_{par} is $7 + 1 + N$. At $N = 16$ the number of parameters per experiment, N_{par}/N is 1.5.

Tests on the reliability of the results

As outlined in the Introduction, the usual statistical tests can be misleading in works based on thermal analysis experiments. Instead, we checked how the evaluation of smaller numbers of experiments affect the results. For this purpose, the evaluations were also carried out on three smaller data-sets which consisted of:

- (i) The modulated and the $20 \text{ }^\circ\text{C min}^{-1}$ experiments (two experiments per sample, eight experiments per least squares evaluation);
- (ii) The modulated and the CRR experiments (two experiments per sample, eight experiments per least squares evaluation);
- (iii) The modulated experiments only (one experiment per sample, four experiments per least squares evaluation).

The E , $reldev_N$, and N_{par}/N values obtained in this way are listed in rows 2–4 in Table 1. The activation energies

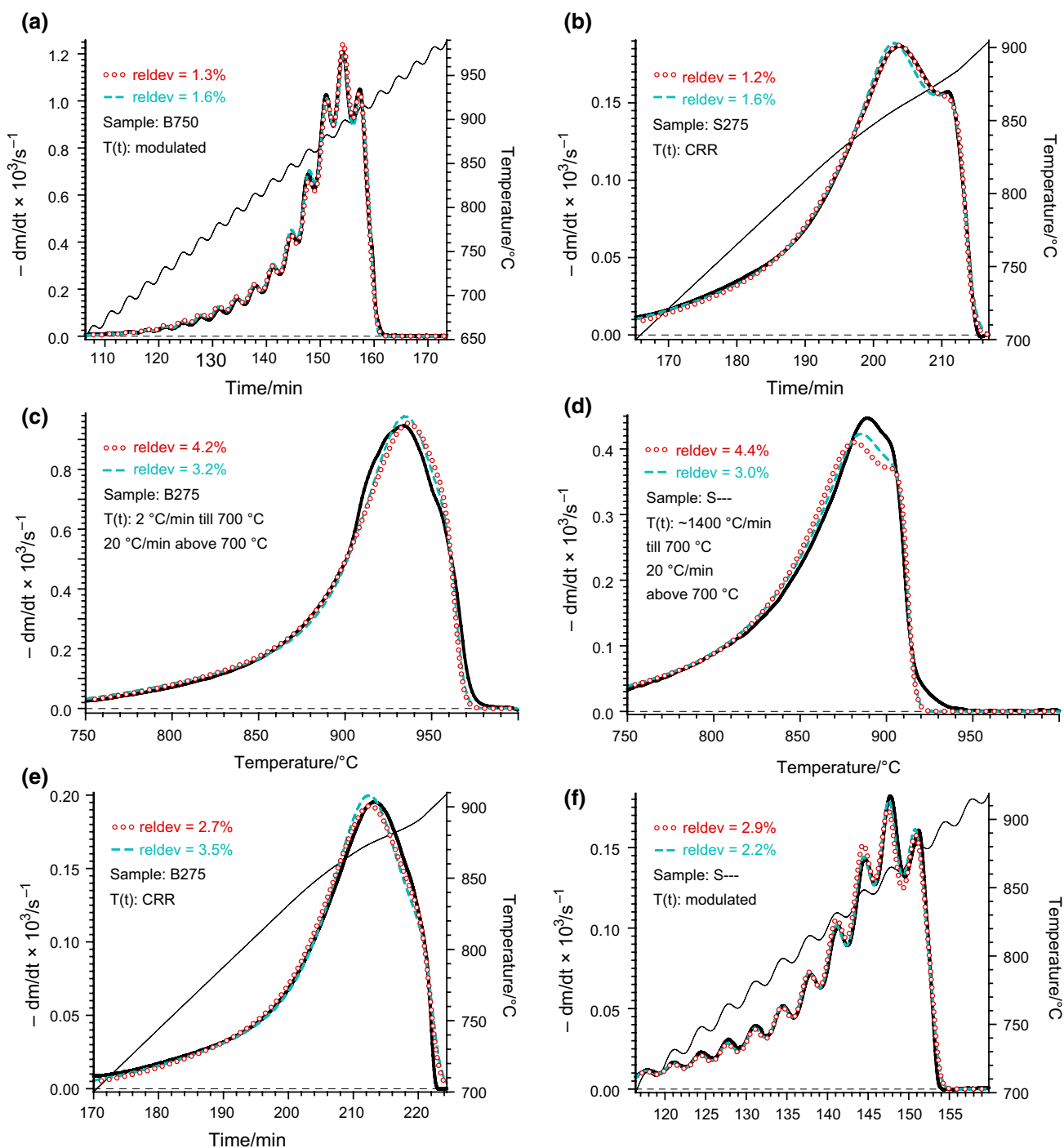


Fig. 1 The best, the worst and a typical fit quality for the birch and the spruce samples in evaluation [2 $f(X)$; 2 E]. The corresponding results from evaluation [8 $f(X)$; 2 E] are also displayed in the figure.

exhibit some scatter. The highest alteration from the average is the $E = 293 \text{ kJ mol}^{-1}$ value in the third row which is 5% higher than the corresponding mean value. This is not a

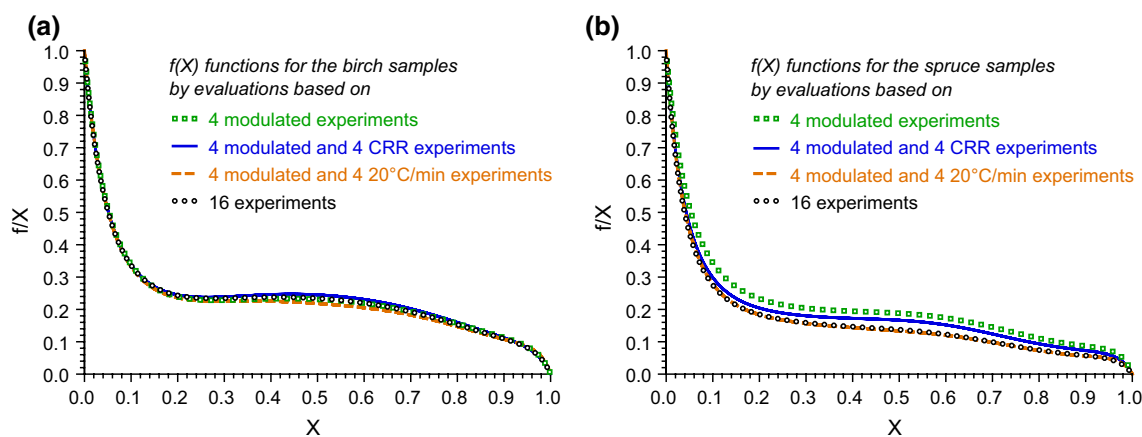
Notation: Thick solid lines: $(-dm/dt)^{\text{obs}}$; thin solid line, when present: $T(t)$; circles and dashed lines: $(-dm/dt)^{\text{calc}}$ curves for evaluations [2 $f(X)$; 2 E] and [8 $f(X)$; 2 E], respectively

considerable difference [11, 39]. The $f(X)$ functions determined from the various subgroups of the experiments are reasonably close to each other, as shown in Fig. 2.

Table 1 Evaluation of various groups of the experiments by assuming separate E values for the birch and spruce samples

Evaluation	Experiments	Birch samples		Spruce samples			
		E	$reldev_N$	E	$reldev_N$	N	N_{par}/N
		kJ mol^{-1}	%	kJ mol^{-1}	%		
$[2 f(X); 2 E]$	All	277	2.6	290	2.8	16	1.5
	mod. & $20\text{ }^\circ\text{C min}^{-1}$	267	2.1	268	2.4	8	2.0
	mod. & CRR	280	1.9	293	2.2	8	2.0
	mod	270	1.6	264	2.0	4	3.0
$[8 f(X); 2 E]$	All	266	2.3	282	2.1	16	2.8
	mod. & $20\text{ }^\circ\text{C min}^{-1}$	268	1.5	267	1.9	8	4.6
	mod. & CRR	274	1.5	285	1.4	8	4.6
	mod	270	1.1	268	1.5	4	8.3
Average E		272		277			
Std. deviation		5 (2%)		12 (4%)			

N is the number of the experiments in the given evaluation. “mod.” is an abbreviation for modulated temperature program

**Fig. 2** The $f(X)$ functions obtained by $[2 f(X); 2 E]$ evaluations for various subgroups of experiments

Determining an $f(X)$ function for each sample

In another series of evaluations, separate $f(X)$ functions were determined for each sample. Altogether eight $f(X)$ functions and two E values were obtained in this way, hence the corresponding notation is $[8 f(X); 2 E]$. The purpose of this part of the work was: (i) To obtain information on the behavior of the samples; and (ii) To continue the reliability tests outlined above. These evaluations were also carried out on different subsets of experiments by the method of least squares. The kinetic parameters determined in an evaluation consisted of one E , N pre-exponential factors, and 4×7 polynomial coefficients for the four $f(X)$ functions. Table 1 contains the corresponding E , $reldev_N$, N , and N_{par}/N values. The dashed lines in Fig. 1 correspond to this evaluation.

Though N_{par}/N varied from 1.5 to 8.3 in Table 1, only a moderate scattering of the E values was observed. The averages and standard deviations of the listed E values are

also shown in Table 1. The standard deviations expressed as percent of the corresponding average are 2% for birch and 4% for spruce.

The $f(X)$ functions determined in the $[8 f(X); 2 E]$ evaluations are shown in Fig. 3. The $f(X)$ functions obtained for a given sample are remarkably similar in Figs. 3a–3h, though there were some moderate differences in the middle part of the X domain in the case of sample B275. All $f(X)$ curves in Figs. 2 and 3 start with a sharp decrease till around $X=0.15$. The last phase of the pyrolysis/devolatilization may contribute to this decrease. However, the $f(X)$ curves for samples B750 and S750 also started with a notable short decrease though these samples were prepared at $750\text{ }^\circ\text{C}$ and they are not supposed to devolatilize below $750\text{ }^\circ\text{C}$. Accordingly, the rapid gasification of the most reactive parts of the samples is probably a major factor in the initial decrease of the $f(X)$ functions. In our opinion the similarities observable in Figs. 2 and 3 affirm the reliability of the results.

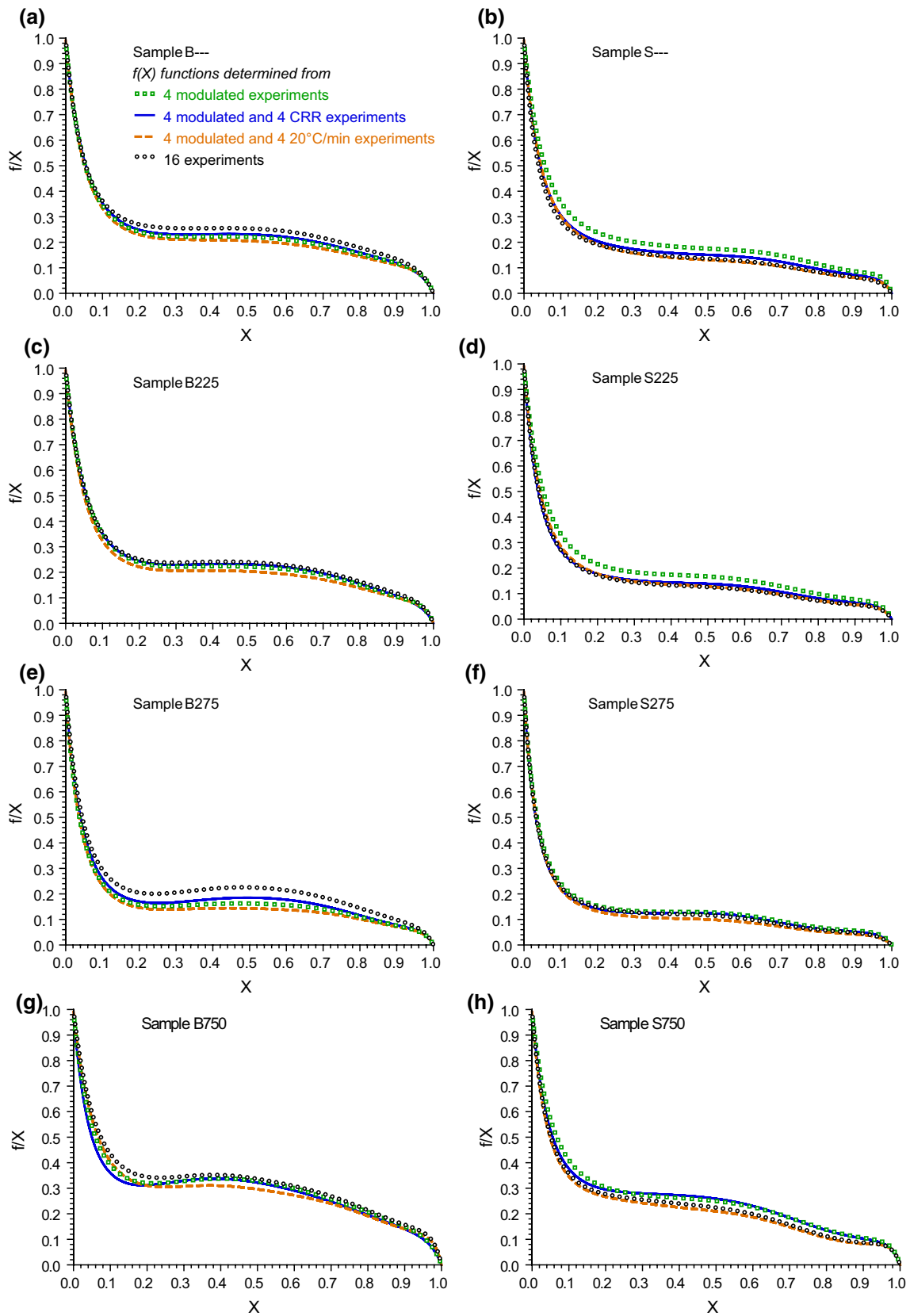


Fig. 3 The $f(X)$ functions obtained in evaluations $[8 f(X); 2 E]$ from different groups of experiments. (Notation: See in Fig. 3a.)

Kinetics with common E and common $f(X)$ for all samples

The mean activation energies of the birch and spruce samples did not differ significantly in Table 1. The $f(X)$ functions determined for the birch and spruce samples are also similar in Figs. 2 and 3. Based on these observations an evaluation was carried out by assuming one E value and one $f(X)$ function for all experiments on all samples. This evaluation is denoted by $[1 f(X); 1 E]$. The corresponding E , $reldev_N$, and N_{par}/N values are listed in Table 2. The standard deviation of E is 0.8% of the corresponding average while the highest difference from the mean is 1.1% in Table 2. The $f(X)$ functions obtained in this way are also close to each other, as Fig. 4 shows. The corresponding fit qualities are illustrated in Fig. S1 of the Supplementary Information.

The usefulness of evaluation $[1 f(X); 1 E]$ is twofold:

- (i) The corresponding results indicate that it is possible to find common E and $f(X)$ for different woods in a wide range of thermal pretreatments.
- (ii) The effects of the feedstock, thermal pretreatments, and heating programs on the gasification reactivity can easily be assessed by the pre-exponential factor values because everything else is common for all samples and all experiments in the $[1 f(X); 1 E]$ evaluation.

The pre-exponential factors are listed and compared in Tables S1 and S2 of the Supplementary Information. The comparison of the pre-exponential factors gives the reactivity differences quantitatively. (Contrary to the traditional comparisons of the peak temperatures for example). For instance, a difference of 0.18 in the $\log_{10} A$ values in Table S1 correspond to difference by a factor of 1.5 in the reaction rates. Besides, such comparisons are applicable for nonlinear temperature programs, as well. In this way the data of Table S1 indicate that the deactivation of the

Table 2 Evaluation of various groups of the experiments by assuming common E and common $f(X)$ for all samples

Experiments	E kJ mol ⁻¹	$reldev_N$ %	N	N_{par}/N
All	271	3.7	32	1.3
mod. & 20 °C min ⁻¹	269	3.2	16	1.5
mod. & CRR	272	3.4	16	1.5
mod	267	2.8	8	2.0
Average E	270			
Std. deviation	2 (1%)			

N is the number of the experiments in the given evaluation. “mod.” is an abbreviation for modulated temperature program

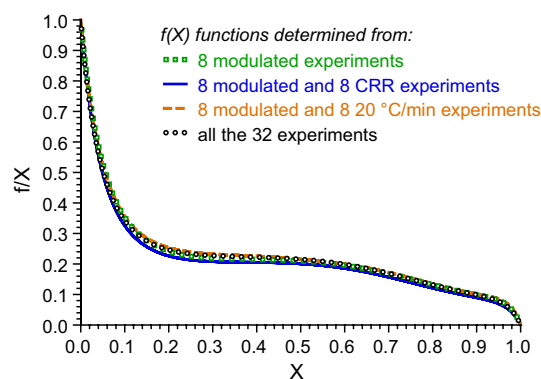


Fig. 4 The $f(X)$ functions obtained by $[1 f(X); 1 E]$ evaluations for various subgroups of experiments

chars is more expressed for the modulated temperature programs than for the roughly four times faster linear heating at 20 °C min⁻¹. It is worth observing in Tables S1 and S2 that the spruce samples are more reactive than the birch samples, though the actual differences vary. The difference is the highest between the reactivities of samples B750 and S750. See further comparisons and explanations in the Supplementary Information.

One-by-one evaluation of the modulated experiments

As a further test, we evaluated the experiments with modulated temperature programs one-by-one by the method of least squares. The notation for this evaluation is $[8 f(X); 8 E]$ which expresses that there is an $f(X)$ function and an E value for each of the eight samples. It is well known that the activation energy can be determined from a single modulated experiment without any assumption on the corresponding $f(X)$ function [40], and there is even an ASTM standard for this procedure [41]. In the present case, however, we determined nine kinetic parameters from one modulated experiment: E , A and the seven parameters of $f(X)$. Nevertheless,

Table 3 The activation energies determined from the eight modulated experiments

Evaluation	E kJ mol ⁻¹	N_{par}/N
$[8 f(X); 8 E]$	271 ± 14	9.0
$[8 f(X); 2 E]$	270 and 268	8.3
$[8 f(X); 1 E]$	269	8.1
$[2 f(X); 2 E]$	270 and 264	3.0
$[2 f(X); 1 E]$	267	2.9
$[1 f(X); 1 E]$	267	2.0
Average E	268	

we got activation energies and $f(X)$ functions reasonably close to the ones determined by the other evaluations from the same experiments. These evaluations resulted in an average E of 271 kJ mol⁻¹ with a standard deviation of 14 kJ mol⁻¹. The latter value is 5% of the mean, which is only a moderate scatter in non-isothermal kinetics [11, 39]. However, this scatter is not a random noise, as will be shown later in this section.

Table 3 gives an overview on the activation energies obtained from the eight modulated experiments in the evaluations of this work. The results obtained in evaluations [8 $f(X)$; 2 E], [2 $f(X)$; 2 E], and [1 $f(X)$; 1 E] are repeated here from Tables 1 and 2 while evaluations [8 $f(X)$; 1 E] and [2 $f(X)$; 1 E] has not yet been included into the treatment. The mean E obtained in the [8 $f(X)$; 8 E] evaluations (271 kJ mol⁻¹) is not far from the other E values in Table 3 which range from 264 till 270 kJ mol⁻¹. The last row contains the averages of the E values listed in Table 3, 268 kJ mol⁻¹. The farthest value from the average in the table is 264 kJ mol⁻¹, its distance from the average is only 1.5%. The number of parameters per experiment, N_{par}/N varies from 2 to 9 in the table. A usual kinetic compensation effect [42] was observed between the E and the $\ln A$ values of the [8 $f(X)$; 8 E] evaluation with “isoconversional temperatures” around 704 °C. However, another compensation effect was also observed between the E values and the characteristics of the obtained $f(X)$ curves that will be outlined below.

The first three rows in Table 3 correspond to evaluations that provided separate $f(X)$ functions the samples. These $f(X)$ functions are compared in Fig. 5. Note that the $f(X)$ functions determined in evaluation [8 $f(X)$; 2 E] from the modulated experiments are shown in Fig. 2, too, hence they are represented by the same line style (by squares) in Figs. 2 and 5 to orient the readers. The activation energy values in evaluation [8 $f(X)$; 8 E] are displayed in Fig. 5 for the easier interpretation of the results.

The main characteristics of the $f(X)$ functions are similar in all figures of this paper: a sharp decrease followed by a longer plateau, as it was mentioned already in the paper. The $f(X)$ curves fit to each other well in Fig. 5a and 5b. This is due to the close activation energy values. In Fig. 5c–5h, however, a compensation effect can be observed: the plateau section is lower when E is higher and vice versa. The one-by-one evaluation of the modulated experiments provides obviously the best fit. When the assumption of an E common to several samples alters E from its best fitting value, the change of E is accompanied by a change of all other kinetic parameters, too, so that the fit between the experimental and calculated data could remain good. This might be the cause of the compensation effect observable in Fig. 5c–5h. A deeper analysis of these effects was out of the scope of the present work; we plan to return to these points in a further

work. Note that the numerical finding of the best fit is more difficult when marked compensation effects exist between the parameters and requires proper parameter transformations [43]. The methods used in the computations of the present work are described in Sect. 4 of the Supplementary Information.

A closer look on the E values in Fig. 5 reveals that they depend on the thermal pretreatment of the samples. The E values of the samples torrefied at 225 °C, B225 and S225 are lower than the average: 259 and 246 kJ mol⁻¹. On the other hand, the E values of the samples torrefied at 275 °C, B275 and S275 are higher than the average: 281 and 290 kJ mol⁻¹. The chars prepared at 750 °C, B750 and S750 also exhibited slightly elevated activation energies, 281 and 277 kJ mol⁻¹, respectively. Accordingly, a major part of the spread of the E values is probably not random. However, the differences between the E values in Fig. 5 are not particularly high. The lowest and the highest E values in Fig. 5 (246 and 290 kJ mol⁻¹) differ by 9 and 7% from the average E .

Keeping the above considerations in mind, we can conclude that the one-by-one evaluation of the modulated experiments by the methods of the present work gave realistic results which are not far from the ones determined from larger groups of experiments by various assumptions.

Comparison of the results to earlier work

As mentioned in the Introduction, the literature of char gasification contains a wide range of controversial kinetic data. It is hard to make a meaningful comparison of the obtained results with the ones published in the literature. On the other hand the experiments treated in the present work have already been evaluated by similar least squares procedures earlier, though less flexible $f(X)$ functions were employed then [19]. The spruce samples were evaluated by n-order kinetics while a two-parameter $f(X)$ function was employed for the birch samples. Neither of those models was capable to mimic the shapes of the $f(X)$ functions determined in the present paper. Note that the $f(X)$ functions of the present work can follow a particularly wide range of shapes [30, 32, 33]. Table 3 in the work of Wang et al., 2014 [19] contains evaluations that were denoted as “all birch samples together” and “all spruce samples together” and aimed to determine a common $f(X)$ function and a common activation energy for the 16 experiments belonging to a given feedstock. The corresponding $reldev_{16}$ values were 5.5 and 4.5%, respectively. In the present work the [2 $f(X)$; 2 E] evaluation of the same experiments resulted in $reldev_{16}$ values of 2.6 and 2.8%, respectively, as shown in Table 1. The closer fit indicates that the calculated curves of the present work could follow better the finer details of the experimental curves. Probably the information contained in the experiments can

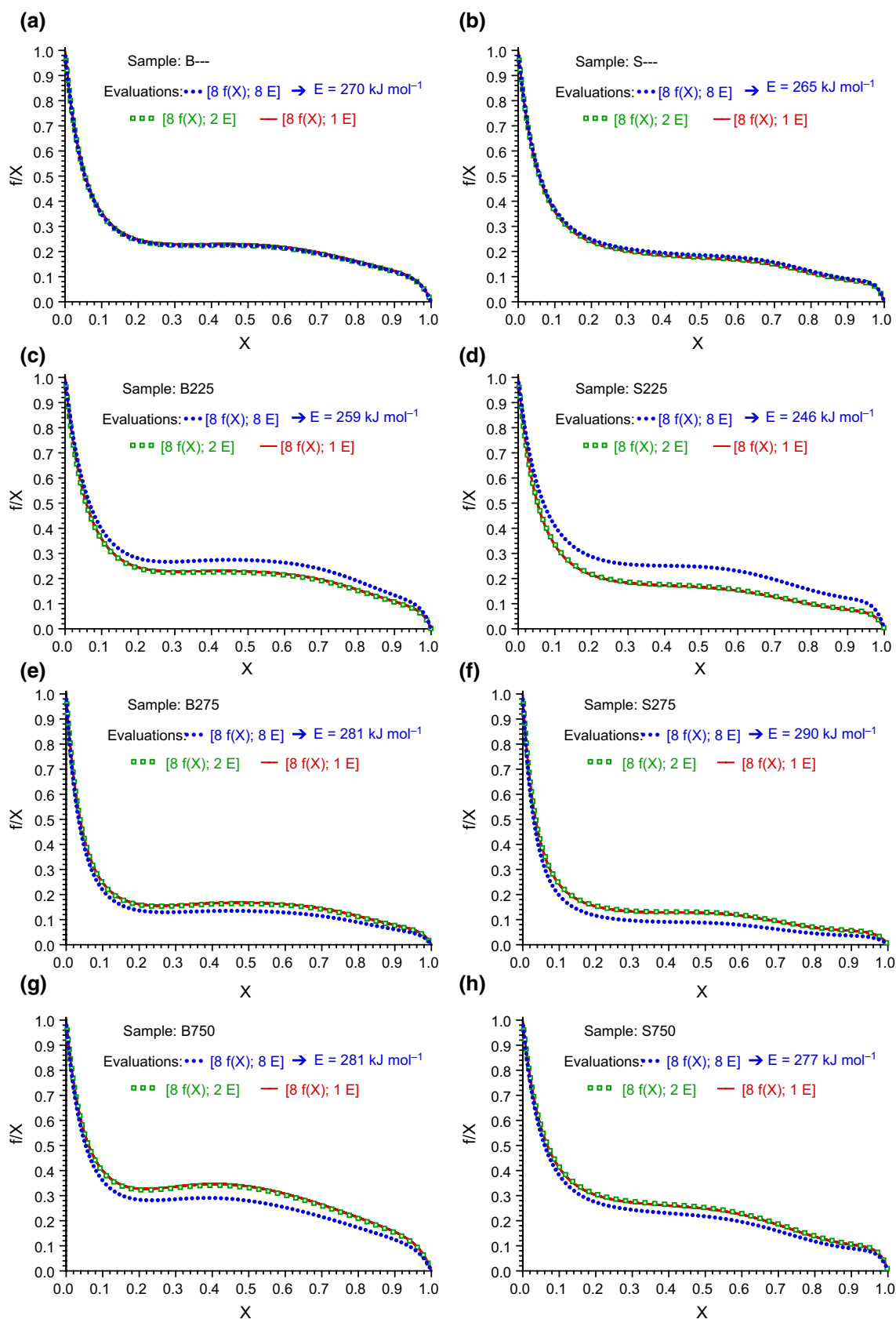


Fig. 5 The $f(X)$ functions obtained from the experiments with modulated temperature program in evaluations $[8 f(X); 8 E]$, $[8 f(X); 2 E]$, and $[8 f(X); 1 E]$. The activation energy values obtained in $[8 f(X); 8 E]$ are indicated in the figure for each sample. (See the text for explanations.)

be better exploited if the model deals with the finer details of the experimental curves, too.

Conclusions

The applicability and reliability of a modelling approach proposed in 2019 [30] were studied. Earlier experiments were reevaluated by this newer tool. Groups of experiments were evaluated together by the method of least squares. The main findings are summarized below.

- (1) Suitable models were found that described well the gasification of chars forming from woods through a wide range of temperature histories.
- (2) The reliability of the results was studied by evaluating different groups of the available experiments. Evaluations based on 4, 8, 16 and 32 experiments resulted in similar E values and $f(X)$ functions.
- (3) The method proved to be suitable for the one-by-one evaluation of the modulated experiments by the method of least squares. It is well known that a single modulated experiment is suitable for the estimation of the activation energy without any assumption on the model function. In the present case, however, a model function, too, was determined for a modulated experiment. The results obtained in this way were similar to the results obtained from larger groups of experiments.
- (4) In other calculations common activation energy and $f(X)$ function were found for a group of samples/experiments. In these cases, the pre-exponential factors expressed the reactivity differences that were caused by the effects of the feedstock, the pretreatments, and the temperature programs of the TGA experiments.
- (5) Besides the usual kinetic compensation effect between E and $\ln A$, another compensation effect was also observed that connected the E values and the characteristics of the obtained $f(X)$ curves.
- (6) The work supplied further evidence about the favorable properties, applicability, and usefulness of the examined way of modelling.

Supplementary Information The online version contains supplementary material available at <https://doi.org/10.1007/s10973-023-12151-y>.

Acknowledgements The authors are grateful for the financial support of the Research Council of Norway and several industrial partners through the project BioCarbUp (“Optimising the biocarbon value chain for sustainable metallurgical industry”, Project Number 294679/E20).

Author contributions GV Conceptualization; methodology; software; writing of the original draft. LW Investigation; resources; review and editing of the manuscript. ØS Supervision; project administration; funding acquisition; review and editing of the manuscript.

Funding Open access funding provided by ELKH Research Centre for Natural Sciences.

Declarations

Conflict of Interest The authors declare that they have no known competing financial interests or personal relationships that could have appeared to influence the work reported in this paper.

Open Access This article is licensed under a Creative Commons Attribution 4.0 International License, which permits use, sharing, adaptation, distribution and reproduction in any medium or format, as long as you give appropriate credit to the original author(s) and the source, provide a link to the Creative Commons licence, and indicate if changes were made. The images or other third party material in this article are included in the article's Creative Commons licence, unless indicated otherwise in a credit line to the material. If material is not included in the article's Creative Commons licence and your intended use is not permitted by statutory regulation or exceeds the permitted use, you will need to obtain permission directly from the copyright holder. To view a copy of this licence, visit <http://creativecommons.org/licenses/by/4.0/>.

References

1. Cortazar M, Lopez G, Alvarez J, Arregi A, Amutio M, Bilbao J, Olazar M. Experimental study and modeling of biomass char gasification kinetics in a novel thermogravimetric flow reactor. *Chem Eng J*. 2020;396:125200. <https://doi.org/10.1016/j.cej.2020.125200>.
2. Schneider C, Walker S, Phounglamcheik A, Umeki K, Kolb T. Effect of calcium dispersion and graphitization during high-temperature pyrolysis of beech wood char on the gasification rate with CO₂. *Fuel*. 2021;283:118826. <https://doi.org/10.1016/j.fuel.2020.118826>.
3. Vamvuka D, Karouki E, Sfakiotakis S. Gasification of waste biomass chars by carbon dioxide via thermogravimetry. Part I: Effect of mineral matter. *Fuel*. 2011;90(3):1120–7. <https://doi.org/10.1016/j.fuel.2010.12.001>.
4. Liu Z, Singer S, Tong Y, Kimbell L, Anderson E, Hughes M, Zitomer D, McNamara P. Characteristics and applications of biochars derived from wastewater solids. *Renew Sustain Energy Rev*. 2018;90:650–64. <https://doi.org/10.1016/j.rser.2018.02.040>.
5. Wang L, Sandquist J, Várhegyi G, Matas GB. CO₂ gasification of chars prepared from wood and forest residue: a kinetic study. *Energy Fuels*. 2013;27:6098–107. <https://doi.org/10.1021/ef3019222>.
6. Roncancio R, Gore JP. CO₂ char gasification: a systematic review from 2014 to 2020. *Energy Conv Manag*. 2021;10:100060. <https://doi.org/10.1016/j.ecmx.2020.100060>.
7. Di Blasi C. Combustion and gasification rates of lignocellulosic chars. *Prog Energy Combust Sci*. 2009;35:121–40. <https://doi.org/10.1016/j.peccs.2008.08.001>.
8. Lahijani P, Zainal ZA, Mohammadi M, Mohamed AR. Conversion of the greenhouse gas CO₂ to the fuel gas CO via the Boudouard reaction: a review. *Renew Sustain Energy Rev*. 2015;41:615–32. <https://doi.org/10.1016/j.rser.2014.08.034>.
9. Trubetskaya A. Reactivity effects of inorganic content in biomass gasification: a review. *Energies*. 2022;15:3137. <https://doi.org/10.3390/en15093137>.
10. Vyazovkin S, Burnham AK, Criado JM, Pérez-Maqueda LA, Popescu C, Sbirrazzuoli N. ICTAC Kinetics Committee recommendations for performing kinetic computations on thermal

- analysis data. *Thermochim Acta*. 2011;520:1–9. <https://doi.org/10.1016/j.tca.2011.03.034>.
11. Vyazovkin S, Burnham AK, Favregeon L, Koga N, Moukhina E, Pérez-Maqueda LA, Sbirrazzuoli N. ICTAC kinetics committee recommendations for analysis of multi-step kinetics. *Thermochim Acta*. 2020;689:178597. <https://doi.org/10.1016/j.tca.2020.178597>.
 12. Bhatia SK, Perlmutter DD. A random pore model for fluid–solid reactions: I Isothermal kinetic control. *AIChE J*. 1980;26:379–86. <https://doi.org/10.1002/aic.690260308>.
 13. Gavalas GR. A random capillary model with application to char gasification at chemically controlled rates. *AIChE J*. 1980;26:577–85. <https://doi.org/10.1002/aic.690260408>.
 14. Chew JJ, Soh M, Sunarso J, Yong S-T, Doshi V, Bhattacharya S. Isothermal kinetic study of CO₂ gasification of torrefied oil palm biomass. *Biomass Bioenergy*. 2020;134:105487. <https://doi.org/10.1016/j.biombioe.2020.105487>.
 15. Sher F, Iqbal SZ, Liu H, Imran M, Snape CE. Thermal and kinetic analysis of diverse biomass fuels under different reaction environment: a way forward to renewable energy sources. *Energy Convers Manag*. 2020;203:112266. <https://doi.org/10.1016/j.biombioe.2020.105487>.
 16. Compendium of Chemical Terminology, Gold Book, version 2.3.3. International Union of Pure and Applied Chemistry, 2014, <https://goldbook.iupac.org/terms/view/A00102> (Retrieved 21 September 2022.)
 17. Várhegyi G, Szabó P, Jakab E, Till F, Richard J-R. Mathematical modeling of char reactivity in Ar-O₂ and CO₂-O₂ mixtures. *Energy Fuels*. 1996;10:208–14. <https://doi.org/10.1021/ef950252z>.
 18. Várhegyi G. Aims and methods in non-isothermal reaction kinetics. *J Anal Appl Pyrolysis*. 2007;79:278–88. <https://doi.org/10.1016/j.jaap.2007.01.007>.
 19. Wang L, Várhegyi G, Skreiberg Ø. CO₂ Gasification of torrefied wood: a kinetic study. *Energy Fuels*. 2014;28:7582–90. <https://doi.org/10.1021/ef502308e>.
 20. Wang L, Li T, Várhegyi G, Skreiberg Ø, Løvås T. CO₂ Gasification of chars prepared by fast and slow pyrolysis from wood and forest residue: a kinetic study. *Energy Fuels*. 2018;32:588–97. <https://doi.org/10.1021/acs.energyfuels.7b03333>.
 21. Tomaszewicz M, Tomaszewicz G, Sciazko M. Experimental study on kinetics of coal char–CO₂ reaction by means of pressurized thermogravimetric analysis. *J Therm Anal Calorim*. 2017;130:2315–30. <https://doi.org/10.1007/s10973-017-6538-3>.
 22. Fernandez-Lopez M, López-González D, Valverde JL, Sanchez-Silva L. Kinetic study of the CO₂ gasification of manure samples. *J Therm Anal Calorim*. 2017;127:2499–509. <https://doi.org/10.1007/s10973-016-5871-2>.
 23. Yao X, Yu Q, Wang K, Xie H, Qin Q. Kinetic study on recovery heat of granulated blast-furnace slag through biomass gasification using CO₂ as gasification agent. *J Therm Anal Calorim*. 2017;131:1313–21. <https://doi.org/10.1007/s10973-017-6670-0>.
 24. Uwaoma RC, Strydom CA, Matjie RH, Bunt JR. Gasification of chars from tetralin liquefaction of <1.5 g cm⁻³ carbon-rich residues derived from waste coal fines in South Africa. *J Therm Anal Calorim*. 2022;147:2353–67. <https://doi.org/10.1007/s10973-021-10609-5>.
 25. Zhang X, Ma M, Bai Y, Song X, Wang J, Lv P, Yu G. Study on high temperature gasification kinetics of coal char by TGA and in situ heating stage microscope. *J Therm Anal Calorim*. 2022;147:8997–9008. <https://doi.org/10.1007/s10973-022-11195-w>.
 26. Naredi P, Yeboah YD, Pisupati SV. Effect of furnace purging on kinetic rate parameter determination using isothermal thermogravimetric analysis. *Energy Fuels*. 2011;25:4937–43. <https://doi.org/10.1021/ef200949n>.
 27. Zhang Q, Yuan Q, Wang H, Wang Z, Yu Z, Liang L, Fang Y, Huang W. Evaluation of gas switch effect on isothermal gas-solid reactions in a thermogravimetric analyzer. *Fuel*. 2019;239:1173–8. <https://doi.org/10.1016/j.fuel.2018.11.101>.
 28. Burnham AK. Obtaining reliable phenomenological chemical kinetic models for real-world applications. *Thermochim Acta*. 2014;597:35–40. <https://doi.org/10.1016/j.tca.2014.10.006>.
 29. Várhegyi G, Wang L, Skreiberg Ø. Towards a meaningful non-isothermal kinetics for biomass materials and other complex organic samples. *J Therm Anal Calorim*. 2018;133:703–12. <https://doi.org/10.1007/s10973-017-6893-0>.
 30. Várhegyi G. Empirical models with constant and variable activation energy for biomass pyrolysis. *Energy Fuels*. 2019;33:2348–58. <https://doi.org/10.1021/acs.energyfuels.9b00040>.
 31. Várhegyi G, Wang L, Skreiberg Ø. Non-isothermal kinetics: best-fitting empirical models instead of model-free methods. *J Therm Anal Calorim*. 2020;142:1043–54. <https://doi.org/10.1007/s10973-019-09162-z>.
 32. Várhegyi G, Wang L, Skreiberg Ø. Empirical kinetic models for the combustion of charcoals and biomasses in the kinetic regime. *Energy Fuels*. 2020;34:16302–9. <https://doi.org/10.1021/acs.energyfuels.0c03248>.
 33. Várhegyi G, Wang L, Skreiberg Ø. Empirical kinetic models for the CO₂ gasification of biomass chars. Part I Gasification of wood chars and forest residue chars. *ACS Omega*. 2021;6:27552–60. <https://doi.org/10.1021/acsomega.1c04577>.
 34. Šimon P, Dubaj T, Cibulková Z. Frequent flaws encountered in the manuscripts of kinetic papers. *J Therm Anal Calorim*. 2022;147(18):10083–8. <https://doi.org/10.1007/s10973-022-11436-y>.
 35. Antal MJ Jr, Grønli M. The art, science, and technology of charcoal production. *Ind Eng Chem Res*. 2003;42:1619–40. <https://doi.org/10.1021/ie0207919>.
 36. Press WH, Flannery BP, Teukolsky SA, Vetterling WT. Numerical Recipes. The Art of Scientific Computing. Cambridge: Cambridge University Press; 2007.
 37. Salatino P, Senneca O, Masi S. Assessment of thermodeactivation during gasification of a bituminous coal char. *Energy Fuels*. 1999;13:1154–9. <https://doi.org/10.1021/ef9900334>.
 38. Holland T, Fletcher TH, Senneca O. Review of carbonaceous annealing effects on O₂ and CO₂ coal reactivity. *Energy Fuels*. 2019;33:10415–34. <https://doi.org/10.1021/acs.energyfuels.9b02698>.
 39. Grønli M, Antal MJ, Várhegyi G. A round-robin study of cellulose pyrolysis kinetics by thermogravimetry. *Ind Eng Chem Res*. 1999;38:2238–44. <https://doi.org/10.1021/ie980601n>.
 40. Blaine RL, Hahn GK. Obtaining kinetic parameters by modulated thermogravimetry. *J Thermal Anal*. 1998;54:695–704. <https://doi.org/10.1023/A:1010171315715>.
 41. ASTM E2958–19: Standard test methods for kinetic parameters by factor jump/modulated thermogravimetry, ASTM International, USA; 2019. <https://doi.org/10.1520/E2958-21>
 42. Brown ME, Galwey AK. The significance of “compensation effects” appearing in data published in “computational aspects of kinetic analysis”: ICTAC project, 2000. *Thermochim Acta*. 2002;387:173–83.
 43. Várhegyi G, Jakab E, Antal MJ Jr. Is the Broido - Shafizadeh model for cellulose pyrolysis true? *Energy Fuels*. 1994;8:1345–52. <https://doi.org/10.1021/ef00048a025>.

Publisher's Note Springer Nature remains neutral with regard to jurisdictional claims in published maps and institutional affiliations.